0^+ fully-charmed tetraquark states

Jian-Rong Zhang ⬤

Department of Physics, College of Liberal Arts and Sciences, National University of Defense Technology,
Changsha 410073, Hunan, People's Republic of China

Motivated by the LHCb's new observation of structures in the J/ψ-pair invariant mass spectrum, which could be classified as possible $cc\bar{c}\bar{c}$ tetraquark candidates, we systematically study 0^+ fully-charmed tetraquark states through QCD sum rules. Developing the calculation techniques to fourfold heavy hadronic systems, four different configuration currents with 0^+ are considered, and vacuum condensates up to dimension six are included in the operator product expansion. Finally, the mass values acquired for 0^+ $cc\bar{c}\bar{c}$ tetraquark states agree well with the experimental data of the broad structure, which support that it could be a 0^+ fully-charmed tetraquark state.

I. INTRODUCTION

The topic of the fully-charmed tetraquark state has attracted much attention. For example, a variety of phenomenological models were employed to predict the existence of some states merely made up of four heavy quarks [1–28]. In particular, without any light-quark contamination, fully-charmed tetraquark states are ideal prototypes to refine one's understanding of heavy-quark dynamics.

Recently, the invariant mass spectrum of double J/ψ was researched using proton-proton collision data recorded by the LHCb experiment, which shows a broad structure just above twice the J/ψ mass ranging from 6.2 to 6.8 GeV and a narrower structure around 6.9 GeV referred to as $X(6900)$ [29]. Before long, various investigations were presented to explain them via different approaches [30–57]. To probe a real hadron, one inevitably has to face the sophisticated nonperturbative QCD problem. As one reliable way to evaluate nonperturbative effects, the QCD sum rule [58] is firmly established on the basic theory, and it has been widely applied to hadronic systems (for reviews, see Refs. [59–62] and references therein). In particular, on 0^+ $cc\bar{c}\bar{c}$ tetraquark states, there are some existing works [11,12,31,41,50] on different versions of the QCD sum rules. By comparison, Ref. [11] used a moment QCD sum rule method augmented by fundamental inequalities to explore the doubly hidden-charm/bottom tetraquark states. Working with the finite energy version of the QCD inverse

Laplace sum rules, Ref. [41] investigated doubly hidden scalar heavy molecules and tetraquarks states. In addition, there are some other QCD sum rule analyses of fully heavy-tetraquark states involving condensate contributions up to dimension four in the operator product expansion (OPE), especially choosing the axial-vector–axial-vector configuration current in Ref. [12], paying attention to the scalar's first radial excited states [31], or introducing a relative P wave to the diquark operator of the tetraquark current [50]. Consumingly motivated by the exciting and significant structures observed in the di-J/ψ mass spectrum, we follow the previous QCD sum rule studies [63–65] of hadrons containing one or two heavy quarks and devote ourselves to developing the corresponding calculation techniques to fourfold heavy hadronic systems. We then intend to systematically study 0^+ fully-charmed tetraquark states with QCD sum rules by taking into account four possible configuration currents and calculating condensates up to dimension six.

The paper is organized as follows. After the Introduction, the QCD sum rule is derived for 0^+ fully-charmed tetraquark states in Sec. II, along with numerical analysis and discussion in Sec. III. The last part contains a brief summary.

II. 0^+ FULLY-CHARMED TETRAQUARK STATE QCD SUM RULES

Considering a tetraquark state, its interpolating current can be ordinarily represented by a diquark-antidiquark configuration. Thus, the following forms of currents could be constructed for 0^+ $cc\bar{c}\bar{c}$ tetraquark states with

$$j = (Q_a^T C\gamma_5 Q_b)(\bar{Q}_a \gamma_5 C \bar{Q}_b^T)$$

for the scalar-scalar configuration,

$$j = (Q_a^T C Q_b)(\bar{Q}_a C \bar{Q}_b^T)$$

for the pseudoscalar-pseudoscalar configuration,

$$j = (Q_a^T C \gamma_\mu Q_b)(\bar{Q}_a \gamma^\mu C \bar{Q}_b^T)$$

for the axial-vector–axial-vector (shortened to axial-axial) configuration, and

$$j = (Q_a^T C \gamma_5 \gamma_\mu Q_b)(\bar{Q}_a \gamma^\mu \gamma_5 C \bar{Q}_b^T)$$

for the vector-vector configuration. Here, the index T indicates the matrix transposition, C is the charge conjugation matrix, Q is the heavy charm quark, and a and b are color indices. It needs to point that these overall scalar forms of currents are constructed as existing works mainly taking into consideration that all of their Lorentz indices being contracted. One should note that the situation for the axial-axial and vector-vector could be more complicated when characterizing a scalar state. In a general way, the combination of two objects with spin 1 may have total spin equal to 0, 1, and 2, and the currents for the axial-axial and vector-vector may represent a mixture of spins. To select the spin-0 part of these two currents, one could try to project their correlation functions into the spin-0 state with the help of the appropriate projection operators, which have been introduced in Refs. [66,67].

To derive QCD sum rules, one can start with the two-point correlator

$$\Pi(q^2) = i \int d^4x e^{iq\cdot x} \langle 0|T[j(x)j^\dagger(0)]|0\rangle. \tag{1}$$

In phenomenology, it can be expressed as

$$\Pi(q^2) = \frac{\lambda_H^2}{M_H^2 - q^2} + \frac{1}{\pi} \int_{s_0}^\infty \frac{\text{Im}[\Pi^{\text{phen}}(s)]}{s - q^2} ds, \tag{2}$$

in which M_H is the hadron's mass, s_0 denotes the continuum threshold, and λ_H displays the coupling of the current to the hadron $\langle 0|j|H\rangle = \lambda_H$. Moreover, it can theoretically be rewritten as

$$\Pi(q^2) = \int_{(4m_Q)^2}^\infty \frac{\rho}{s - q^2} ds, \tag{3}$$

where m_Q is the heavy charm mass, and the spectral density $\rho = \frac{1}{\pi}\text{Im}[\Pi(s)]$. After equating Eqs. (2) and (3), adopting quark-hadron duality, and applying a Borel transform, it yields

$$\lambda_H^2 e^{-M_H^2/M^2} = \int_{(4m_Q)^2}^{s_0} \rho e^{-s/M^2} ds, \tag{4}$$

with M^2 the Borel parameter. Taking the derivative of Eq. (4) with respect to $-\frac{1}{M^2}$ and then dividing the result by Eq. (4) itself, one could achieve the mass sum rule

$$M_H = \sqrt{\int_{(4m_Q)^2}^{s_0} \rho s e^{-s/M^2} ds \Big/ \int_{(4m_Q)^2}^{s_0} \rho e^{-s/M^2} ds}. \tag{5}$$

In the OPE calculation, one could work in momentum space making use of the heavy-quark propagator [68], and then the result is dimensionally regularized at $D = 4$ by making an extension of the calculation techniques [63–65] to fully heavy-tetraquark systems. The spectral density is concretely expressed as $\rho = \rho^{\text{pert}} + \rho^{\langle g^2 G^2 \rangle} + \rho^{\langle g^3 G^3 \rangle}$, with

$$\rho^{\text{pert}} = -\frac{1}{2^{10}\pi^6} \int_{\alpha_{\min}}^{\alpha_{\max}} \frac{d\alpha}{\alpha^3} \int_{\beta_{\min}}^{\beta_{\max}} \frac{d\beta}{\beta^3} \int_{\gamma_{\min}}^{\gamma_{\max}} \frac{d\gamma}{\gamma^3} \frac{1}{\mathbf{H}^6} \left[m_Q^2 - \frac{(1 - \alpha - \beta - \gamma)s}{\mathbf{H}} \right]^2$$
$$\times \{ [-3(1 - \alpha - \beta - \gamma) + 4(\gamma(1 - \alpha - \beta - \gamma) + \alpha\beta)\mathbf{H} - 6\alpha\beta\gamma\mathbf{H}^2]\mathbf{H}^2 m_Q^4$$
$$+ (1 - \alpha - \beta - \gamma)[18(1 - \alpha - \beta - \gamma) - 10(\gamma(1 - \alpha - \beta - \gamma) + \alpha\beta)\mathbf{H}]\mathbf{H} m_Q^2 s - 21(1 - \alpha - \beta - \gamma)^3 s^2 \},$$

$$\rho^{\langle g^2 G^2 \rangle} = -\frac{m_Q^2 \langle g^2 G^2 \rangle}{3 \cdot 2^9 \pi^6} \int_{\alpha_{\min}}^{\alpha_{\max}} \frac{d\alpha}{\alpha^3} \int_{\beta_{\min}}^{\beta_{\max}} \frac{d\beta}{\beta^3} \int_{\gamma_{\min}}^{\gamma_{\max}} \frac{d\gamma}{\gamma^3} \frac{(1 - \alpha - \beta - \gamma)^2}{\mathbf{H}^5}$$
$$\times \{ [-6(1 - \alpha - \beta - \gamma)^2 + (1 - \alpha - \beta - \gamma)(6\gamma + 2\gamma(1 - \alpha - \beta - \gamma) + 2\alpha\beta)\mathbf{H} - 3\alpha\beta\gamma\mathbf{H}^2]\mathbf{H} m_Q^2$$
$$+ 3(1 - \alpha - \beta - \gamma)^2 [4(1 - \alpha - \beta - \gamma) - 3\gamma\mathbf{H}]s \},$$

$$\rho^{\langle g^3 G^3 \rangle} = -\frac{\langle g^3 G^3 \rangle}{3 \cdot 2^{10} \pi^6} \int_{\alpha_{\min}}^{\alpha_{\max}} \frac{d\alpha}{\alpha^3} \int_{\beta_{\min}}^{\beta_{\max}} \frac{d\beta}{\beta^3} \int_{\gamma_{\min}}^{\gamma_{\max}} \frac{d\gamma}{\gamma^3} \frac{(1 - \alpha - \beta - \gamma)^3}{\mathbf{H}^5} \{ [-3(1 - \alpha - \beta - \gamma)$$
$$- 6(1 - \alpha - \beta - \gamma)^2 + 6\gamma(1 - \alpha - \beta - \gamma)\mathbf{H} + \alpha\beta\mathbf{H}]\mathbf{H} m_Q^2 + 6(1 - \alpha - \beta - \gamma)^2 s \},$$

for the scalar-scalar current,

$$\rho^{\text{pert}} = -\frac{1}{2^{10}\pi^6} \int_{\alpha_{\min}}^{\alpha_{\max}} \frac{d\alpha}{\alpha^3} \int_{\beta_{\min}}^{\beta_{\max}} \frac{d\beta}{\beta^3} \int_{\gamma_{\min}}^{\gamma_{\max}} \frac{d\gamma}{\gamma^3} \frac{1}{\mathbf{H}^6} \left[m_Q^2 - \frac{(1-\alpha-\beta-\gamma)s}{\mathbf{H}} \right]^2$$
$$\times \{ [-3(1-\alpha-\beta-\gamma) - 4(\gamma(1-\alpha-\beta-\gamma) + \alpha\beta)\mathbf{H} - 6\alpha\beta\gamma\mathbf{H}^2]\mathbf{H}^2 m_Q^4$$
$$+ (1-\alpha-\beta-\gamma)[18(1-\alpha-\beta-\gamma) + 10(\gamma(1-\alpha-\beta-\gamma) + \alpha\beta)\mathbf{H}]\mathbf{H}m_Q^2 s - 21(1-\alpha-\beta-\gamma)^3 s^2 \},$$

$$\rho^{\langle g^2 G^2 \rangle} = -\frac{m_Q^2 \langle g^2 G^2 \rangle}{3 \cdot 2^9 \pi^6} \int_{\alpha_{\min}}^{\alpha_{\max}} \frac{d\alpha}{\alpha^3} \int_{\beta_{\min}}^{\beta_{\max}} \frac{d\beta}{\beta^3} \int_{\gamma_{\min}}^{\gamma_{\max}} \frac{d\gamma}{\gamma^3} \frac{(1-\alpha-\beta-\gamma)^2}{\mathbf{H}^5}$$
$$\times \{ [-6(1-\alpha-\beta-\gamma)^2 - (1-\alpha-\beta-\gamma)(6\gamma + 2\gamma(1-\alpha-\beta-\gamma) + 2\alpha\beta)\mathbf{H} - 3\alpha\beta\gamma\mathbf{H}^2]\mathbf{H}m_Q^2$$
$$+ 3(1-\alpha-\beta-\gamma)^2 [4(1-\alpha-\beta-\gamma) + 3\gamma\mathbf{H}]s \},$$

$$\rho^{\langle g^3 G^3 \rangle} = -\frac{\langle g^3 G^3 \rangle}{3 \cdot 2^{10} \pi^6} \int_{\alpha_{\min}}^{\alpha_{\max}} \frac{d\alpha}{\alpha^3} \int_{\beta_{\min}}^{\beta_{\max}} \frac{d\beta}{\beta^3} \int_{\gamma_{\min}}^{\gamma_{\max}} \frac{d\gamma}{\gamma^3} \frac{(1-\alpha-\beta-\gamma)^3}{\mathbf{H}^5} \{ [-3(1-\alpha-\beta-\gamma)$$
$$- 6(1-\alpha-\beta-\gamma)^2 - 6\gamma(1-\alpha-\beta-\gamma)\mathbf{H} - \alpha\beta\mathbf{H}]\mathbf{H}m_Q^2 + 6(1-\alpha-\beta-\gamma)^2 s \},$$

for the pseudoscalar-pseudoscalar current,

$$\rho^{\text{pert}} = -\frac{1}{2^8 \pi^6} \int_{\alpha_{\min}}^{\alpha_{\max}} \frac{d\alpha}{\alpha^3} \int_{\beta_{\min}}^{\beta_{\max}} \frac{d\beta}{\beta^3} \int_{\gamma_{\min}}^{\gamma_{\max}} \frac{d\gamma}{\gamma^3} \frac{1}{\mathbf{H}^6} \left[m_Q^2 - \frac{(1-\alpha-\beta-\gamma)s}{\mathbf{H}} \right]^2$$
$$\times \{ [-3(1-\alpha-\beta-\gamma) + 2(\gamma(1-\alpha-\beta-\gamma) + \alpha\beta)\mathbf{H} - 6\alpha\beta\gamma\mathbf{H}^2]\mathbf{H}^2 m_Q^4$$
$$+ (1-\alpha-\beta-\gamma)[18(1-\alpha-\beta-\gamma) - 5(\gamma(1-\alpha-\beta-\gamma) + \alpha\beta)\mathbf{H}]\mathbf{H}m_Q^2 s - 21(1-\alpha-\beta-\gamma)^3 s^2 \},$$

$$\rho^{\langle g^2 G^2 \rangle} = -\frac{m_Q^2 \langle g^2 G^2 \rangle}{3 \cdot 2^8 \pi^6} \int_{\alpha_{\min}}^{\alpha_{\max}} \frac{d\alpha}{\alpha^3} \int_{\beta_{\min}}^{\beta_{\max}} \frac{d\beta}{\beta^3} \int_{\gamma_{\min}}^{\gamma_{\max}} \frac{d\gamma}{\gamma^3} \frac{(1-\alpha-\beta-\gamma)^2}{\mathbf{H}^5}$$
$$\times \{ [-12(1-\alpha-\beta-\gamma)^2 + (1-\alpha-\beta-\gamma)(6\gamma + 2\gamma(1-\alpha-\beta-\gamma) + 2\alpha\beta)\mathbf{H} - 6\alpha\beta\gamma\mathbf{H}^2]\mathbf{H}m_Q^2$$
$$+ 3(1-\alpha-\beta-\gamma)^2 [8(1-\alpha-\beta-\gamma) - 3\gamma\mathbf{H}]s \},$$

$$\rho^{\langle g^3 G^3 \rangle} = -\frac{\langle g^3 G^3 \rangle}{3 \cdot 2^9 \pi^6} \int_{\alpha_{\min}}^{\alpha_{\max}} \frac{d\alpha}{\alpha^3} \int_{\beta_{\min}}^{\beta_{\max}} \frac{d\beta}{\beta^3} \int_{\gamma_{\min}}^{\gamma_{\max}} \frac{d\gamma}{\gamma^3} \frac{(1-\alpha-\beta-\gamma)^3}{\mathbf{H}^5} \{ [-6(1-\alpha-\beta-\gamma)$$
$$- 12(1-\alpha-\beta-\gamma)^2 + 6\gamma(1-\alpha-\beta-\gamma)\mathbf{H} + \alpha\beta\mathbf{H}]\mathbf{H}m_Q^2 + 12(1-\alpha-\beta-\gamma)^2 s \},$$

for the axial-axial current, and

$$\rho^{\text{pert}} = -\frac{1}{2^8 \pi^6} \int_{\alpha_{\min}}^{\alpha_{\max}} \frac{d\alpha}{\alpha^3} \int_{\beta_{\min}}^{\beta_{\max}} \frac{d\beta}{\beta^3} \int_{\gamma_{\min}}^{\gamma_{\max}} \frac{d\gamma}{\gamma^3} \frac{1}{\mathbf{H}^6} \left[m_Q^2 - \frac{(1-\alpha-\beta-\gamma)s}{\mathbf{H}} \right]^2$$
$$\times \{ [-3(1-\alpha-\beta-\gamma) - 2(\gamma(1-\alpha-\beta-\gamma) + \alpha\beta)\mathbf{H} - 6\alpha\beta\gamma\mathbf{H}^2]\mathbf{H}^2 m_Q^4$$
$$+ (1-\alpha-\beta-\gamma)[18(1-\alpha-\beta-\gamma) + 5(\gamma(1-\alpha-\beta-\gamma) + \alpha\beta)\mathbf{H}]\mathbf{H}m_Q^2 s - 21(1-\alpha-\beta-\gamma)^3 s^2 \},$$

$$\rho^{\langle g^2 G^2 \rangle} = -\frac{m_Q^2 \langle g^2 G^2 \rangle}{3 \cdot 2^8 \pi^6} \int_{\alpha_{\min}}^{\alpha_{\max}} \frac{d\alpha}{\alpha^3} \int_{\beta_{\min}}^{\beta_{\max}} \frac{d\beta}{\beta^3} \int_{\gamma_{\min}}^{\gamma_{\max}} \frac{d\gamma}{\gamma^3} \frac{(1-\alpha-\beta-\gamma)^2}{\mathbf{H}^5}$$
$$\times \{ [-12(1-\alpha-\beta-\gamma)^2 - (1-\alpha-\beta-\gamma)(6\gamma + 2\gamma(1-\alpha-\beta-\gamma) + 2\alpha\beta)\mathbf{H} - 6\alpha\beta\gamma\mathbf{H}^2]\mathbf{H}m_Q^2$$
$$+ 3(1-\alpha-\beta-\gamma)^2 [8(1-\alpha-\beta-\gamma) + 3\gamma\mathbf{H}]s \},$$

$$\rho^{\langle g^3 G^3 \rangle} = -\frac{\langle g^3 G^3 \rangle}{3 \cdot 2^9 \pi^6} \int_{\alpha_{\min}}^{\alpha_{\max}} \frac{d\alpha}{\alpha^3} \int_{\beta_{\min}}^{\beta_{\max}} \frac{d\beta}{\beta^3} \int_{\gamma_{\min}}^{\gamma_{\max}} \frac{d\gamma}{\gamma^3} \frac{(1-\alpha-\beta-\gamma)^3}{\mathbf{H}^5} \{ [-6(1-\alpha-\beta-\gamma)$$
$$- 12(1-\alpha-\beta-\gamma)^2 - 6\gamma(1-\alpha-\beta-\gamma)\mathbf{H} - \alpha\beta\mathbf{H}]\mathbf{H}m_Q^2 + 12(1-\alpha-\beta-\gamma)^2 s \},$$

for the vector-vector current. It is defined as

$$\mathbf{H} = 1 + (1 - \alpha - \beta - \gamma)\left(\frac{1}{\alpha} + \frac{1}{\beta} + \frac{1}{\gamma}\right),$$

$$\alpha_{\min} = \frac{1}{2}\left[\left(1 - \frac{8m_Q^2}{s}\right) - \sqrt{\left(1 - \frac{8m_Q^2}{s}\right)^2 - \frac{4m_Q^2}{s}}\right],$$

$$\alpha_{\max} = \frac{1}{2}\left[\left(1 - \frac{8m_Q^2}{s}\right) + \sqrt{\left(1 - \frac{8m_Q^2}{s}\right)^2 - \frac{4m_Q^2}{s}}\right],$$

$$\beta_{\min} = \frac{1}{2}\left[\left(1 + 2\alpha - \frac{3\alpha^2 s}{\alpha s - m_Q^2}\right) - \sqrt{\frac{[\alpha(1-\alpha)s - m_Q^2][\alpha(1-\alpha)s - (1+8\alpha)m_Q^2]}{(\alpha s - m_Q^2)^2}}\right],$$

$$\beta_{\max} = \frac{1}{2}\left[\left(1 + 2\alpha - \frac{3\alpha^2 s}{\alpha s - m_Q^2}\right) + \sqrt{\frac{[\alpha(1-\alpha)s - m_Q^2][\alpha(1-\alpha)s - (1+8\alpha)m_Q^2]}{(\alpha s - m_Q^2)^2}}\right],$$

$$\gamma_{\min} = \frac{1}{2}\left[(1 - \alpha - \beta) - \sqrt{\frac{(1-\alpha-\beta)\{(1-\alpha-\beta)[\alpha\beta s - (\alpha+\beta)m_Q^2] - 4\alpha\beta m_Q^2\}}{\alpha\beta s - (\alpha+\beta)m_Q^2}}\right],$$

and

$$\gamma_{\max} = \frac{1}{2}\left[(1 - \alpha - \beta) + \sqrt{\frac{(1-\alpha-\beta)\{(1-\alpha-\beta)[\alpha\beta s - (\alpha+\beta)m_Q^2] - 4\alpha\beta m_Q^2\}}{\alpha\beta s - (\alpha+\beta)m_Q^2}}\right].$$

III. NUMERICAL ANALYSIS AND DISCUSSION

In this section, the heavy m_Q is taken as the running charm mass $m_c = 1.27 \pm 0.02$ GeV [69], and the other input parameters are $\langle g^2 G^2 \rangle = 0.88 \pm 0.25$ GeV^4 and $\langle g^3 G^3 \rangle = 0.58 \pm 0.18$ GeV^6 [58,62,70]. Following the standard criterion of sum rule analysis, one could find proper work windows for the threshold parameter $\sqrt{s_0}$ and the Borel parameter M^2. The lower bound of M^2 can be gained in view of the OPE convergence, and the upper one is obtained from the pole dominance. Meanwhile, the threshold $\sqrt{s_0}$ is around 0.4–0.6 GeV higher than the extracted M_H empirically, which describes the beginning of continuum state.

Taking the scalar-scalar case as an example, the inputs are kept at their central values at the start. To find the lower bound of M^2, its OPE convergence is shown by comparing the relative contributions of various condensates from sum rule (4) for $\sqrt{s_0} = 7.0$ GeV in Fig. 1, and one can note that the relative contributions of two-gluon condensate $\langle g^2 G^2 \rangle$ and three-gluon condensate $\langle g^3 G^3 \rangle$ are very small. Numerically, it is taken as $M^2 \geq 2.5$ GeV^2 with an eye on the OPE convergence analysis. On the other hand, the upper one of M^2 is obtained from the pole contribution dominance phenomenologically. Figure 2 compares the pole and continuum contribution from sum rule (4) for $\sqrt{s_0} = 7.0$ GeV. The relative pole contribution is about

50% at $M^2 = 3.0$ GeV^2 and decreasing with M^2. Thereby, it can satisfy the pole dominance requirement while $M^2 \leq 3.0$ GeV^2, and the Borel window is fixed as $M^2 = 2.5$–3.0 GeV^2 for $\sqrt{s_0} = 7.0$ GeV. Analogously, they are taken as $M^2 = 2.5$–2.9 GeV^2 for $\sqrt{s_0} = 6.9$ GeV, and $M^2 = 2.5$–3.2 GeV^2 for $\sqrt{s_0} = 7.1$ GeV, respectively.
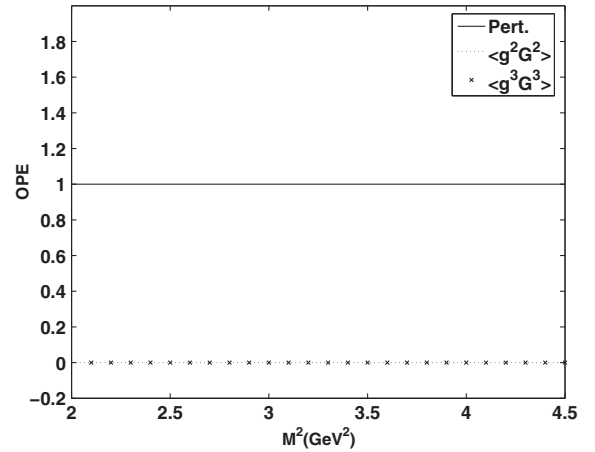

FIG. 1. The OPE convergence for the 0^+ fully-charmed tetraquark state with a scalar-scalar configuration shown by comparing the relative contributions of perturbative two-gluon condensate $\langle g^2 G^2 \rangle$, and three-gluon condensate $\langle g^3 G^3 \rangle$ from sum rule (4) for $\sqrt{s_0} = 7.0$ GeV.
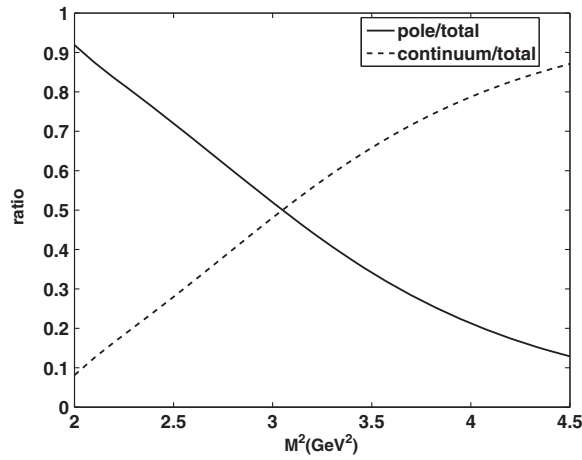
FIG. 2. The phenomenological contribution in sum rule (4) for $\sqrt{s_0} = 7.0$ GeV for the 0^+ fully-charmed tetraquark state with a scalar-scalar configuration. The solid line is the relative pole contribution as a function of M^2, and the dashed line is the relative continuum contribution.

FIG. 4. The mass M_H dependence on M^2 for the 0^+ fully-charmed tetraquark state with a pseudoscalar-pseudoscalar configuration from sum rule (5) is shown. The Borel windows of M^2 are 2.5–2.9 GeV^2 for $\sqrt{s_0} = 6.9$ GeV, 2.5–3.0 GeV^2 for $\sqrt{s_0} = 7.0$ GeV, and 2.5–3.2 GeV^2 for $\sqrt{s_0} = 7.1$ GeV, respectively.

The mass M_H dependence on M^2 is shown in Fig. 3 for the scalar-scalar case, and it is computed as 6.44 ± 0.13 GeV in the chosen windows. Then, varying all the input values, the attained mass is $6.44 \pm 0.13^{+0.02}_{-0.03}$ GeV (the first error is from the variation of s_0 and M^2, and the second is from the uncertainty of the QCD parameters) or $6.44^{+0.15}_{-0.16}$ GeV in a short form.

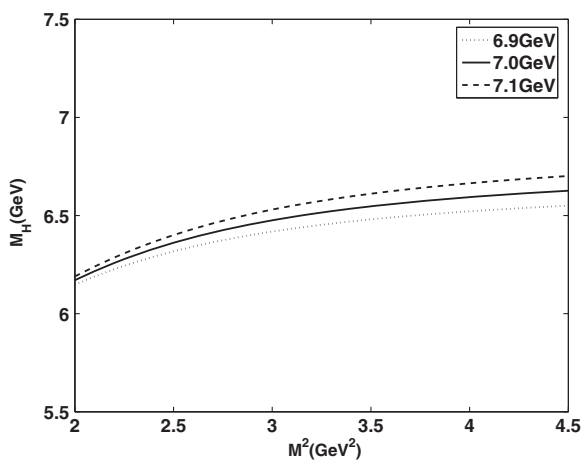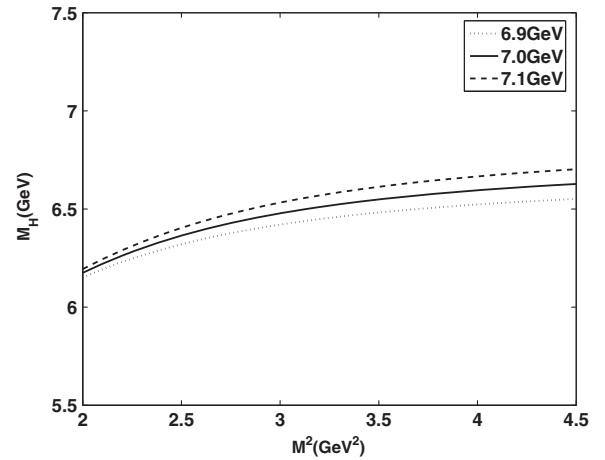In a very similar analysis process, the proper work windows for the other three cases can also be found,

and their corresponding Borel curves are, respectively, given in Figs. 4–6. After considering the uncertainty from both the work windows and the variation of input parameters, the mass values of 0^+ $cc\bar{c}\bar{c}$ tetraquark states are gained as $6.45^{+0.14}_{-0.16}$ GeV for the pseudoscalar-pseudoscalar configuration, $6.46^{+0.13}_{-0.17}$ GeV for the axial-axial configuration, and $6.47^{+0.12}_{-0.18}$ GeV for the vector-vector configuration, respectively.
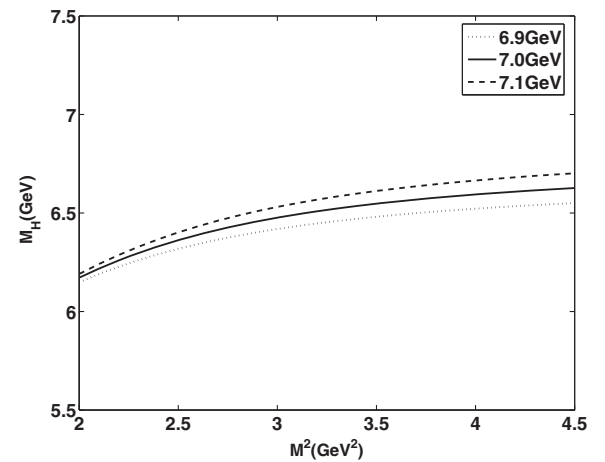

FIG. 3. The mass M_H dependence on M^2 for the 0^+ fully-charmed tetraquark state with a scalar-scalar configuration from sum rule (5) is shown. The Borel windows of M^2 are 2.5–2.9 GeV^2 for $\sqrt{s_0} = 6.9$ GeV, 2.5–3.0 GeV^2 for $\sqrt{s_0} = 7.0$ GeV, and 2.5–3.2 GeV^2 for $\sqrt{s_0} = 7.1$ GeV, respectively.

FIG. 5. The mass M_H dependence on M^2 for the 0^+ fully-charmed tetraquark state with a axial-axial configuration from sum rule (5) is shown. The Borel windows of M^2 are 2.5–2.9 GeV^2 for $\sqrt{s_0} = 6.9$ GeV, 2.5–3.0 GeV^2 for $\sqrt{s_0} = 7.0$ GeV, and 2.5–3.2 GeV^2 for $\sqrt{s_0} = 7.1$ GeV, respectively.
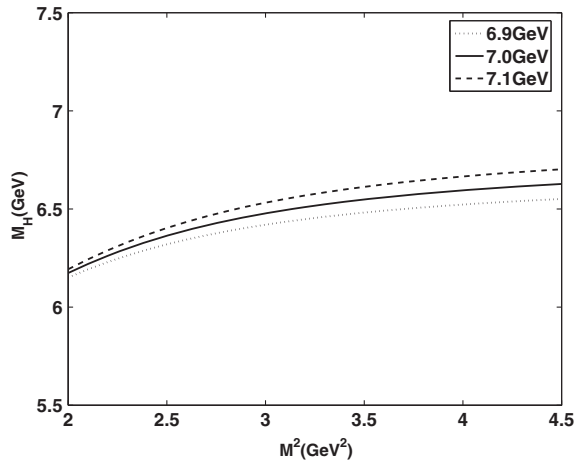
FIG. 6. The mass M_H dependence on M^2 for the 0^+ fully-charmed tetraquark state with a vector-vector configuration from sum rule (5) is shown. The Borel windows of M^2 are 2.5–2.9 GeV^2 for $\sqrt{s_0} = 6.9$ GeV, 2.5–3.0 GeV^2 for $\sqrt{s_0} = 7.0$ GeV, and 2.5–3.2 GeV^2 for $\sqrt{s_0} = 7.1$ GeV, respectively.

IV. SUMMARY

Focusing on the LHCb's new observation in the di-J/ψ mass spectrum, we systematically investigate 0^+ fully-charmed tetraquark states in the framework of QCD sum rules. By developing related calculation techniques for fourfold heavy-tetraquark states, four types of currents with different configurations are taken into consideration, and condensates up to dimension six are involved in the OPE side. Finally, mass values of 0^+ $cc\bar{c}\bar{c}$ tetraquark states are calculated to be $6.44^{+0.15}_{-0.16}$ GeV for the scalar-scalar case, $6.45^{+0.14}_{-0.16}$ GeV for the pseudoscalar-pseudoscalar case, $6.46^{+0.13}_{-0.17}$ GeV for the axial-axial case, and $6.47^{+0.12}_{-0.18}$ GeV for the vector-vector case, respectively. All these results are numerically consistent with the LHCb's experimental data 6.2–6.8 GeV for the broad structure, which could support its internal structure as a 0^+ $cc\bar{c}\bar{c}$ tetraquark state. In the future, it is expected that further experimental and theoretical efforts may reveal more about the nature of the exotic states.

[1] Y. Iwasaki, Phys. Rev. Lett. **36**, 1266 (1976).

[2] K. T. Chao, Z. Phys. C **7**, 317 (1981).

[3] J. P. Ader, J. M. Richard, and P. Taxil, Phys. Rev. D **25**, 2370 (1982).

[4] A. M. Badalian, B. L. Ioffe, and A. V. Smilga, Nucl. Phys. **B281**, 85 (1987).

[5] R. J. Lloyd and J. P. Vary, Phys. Rev. D **70**, 014009 (2004).

[6] N. Barnea, J. Vijande, and A. Valcarce, Phys. Rev. D **73**, 054004 (2006).

[7] A. V. Berezhnoy, A. V. Luchinsky, and A. A. Novoselov, Phys. Rev. D **86**, 034004 (2012).

[8] A. V. Berezhnoy, A. K. Likhoded, and A. A. Novoselov, Phys. Rev. D **87**, 054023 (2013).

[9] M. Karliner, S. Nussinov, and J. L. Rosner, Phys. Rev. D **95**, 034011 (2017).

[10] J. M. Richard, A. Valcarce, and J. Vijande, Phys. Rev. D **95**, 054019 (2017).

[11] W. Chen, H. X. Chen, X. Liu, T. G. Steele, and S. L. Zhu, Phys. Lett. B **773**, 247 (2017).

[12] Z. G. Wang, Eur. Phys. J. C **77**, 432 (2017).

[13] Y. Chen and R. Vega-Morales, arXiv:1710.02738.

[14] J. Wu, Y. R. Liu, K. Chen, X. Liu, and S. L. Zhu, Phys. Rev. D **97**, 094015 (2018).

[15] M. N. Anwar, J. Ferretti, F. K. Guo, E. Santopinto, and B. S. Zou, Eur. Phys. J. C **78**, 647 (2018).

[16] A. Esposito and A. D. Polosa, Eur. Phys. J. C **78**, 782 (2018).

[17] C. Hughes, E. Eichten, and C. T. H. Davies, Phys. Rev. D **97**, 054505 (2018).

[18] V. R. Debastiani and F. S. Navarra, Chin. Phys. C **43**, 013105 (2019).

[19] M. S. Liu, Q. F. Lü, X. H. Zhong, and Q. Zhao, Phys. Rev. D **100**, 016006 (2019).

[20] G. J. Wang, L. Meng, and S. L. Zhu, Phys. Rev. D **100**, 096013 (2019).

[21] M. A. Bedolla, J. Ferretti, C. D. Roberts, and E. Santopinto, Eur. Phys. J. C **80**, 1004 (2020).

[22] Z. G. Wang and Z. Y. Di, Acta Phys. Pol. B **50**, 1335 (2019).

[23] X. Chen, Phys. Rev. D **100**, 094009 (2019).

[24] Y. R. Liu, H. X. Chen, W. Chen, X. Liu, and S. L. Zhu, Prog. Part. Nucl. Phys. **107**, 237 (2019).

[25] Y. Bai, S. Lu, and J. Osborne, Phys. Lett. B **798**, 134930 (2019).

[26] C. Becchi, A. Giachino, L. Maiani, and E. Santopinto, Phys. Lett. B **806**, 135495 (2020).

[27] X. Chen, arXiv:2001.06755.

[28] C. Deng, H. Chen, and J. Ping, Phys. Rev. D **103**, 014001 (2021).

[29] R. Aaij *et al.* (LHCb Collaboration), Sci. Bull. **65**, 1983 (2020).

[30] M. S. Liu, F. X. Liu, X. H. Zhong, and Q. Zhao, arXiv: 2006.11952.

[31] Z. G. Wang, Chin. Phys. C **44**, 113106 (2020).

[32] X. Jin, Y. Xue, H. Huang, and J. Ping, Eur. Phys. J. C **80**, 1083 (2020).

[33] G. Yang, J. Ping, L. He, and Q. Wang, arXiv:2006.13756.

[34] C. Becchi, J. Ferretti, A. Giachino, L. Maiani, and E. Santopinto, Phys. Lett. B **811**, 135952 (2020).

[35] Q. F. Lü, D. Y. Chen, and Y. B. Dong, Eur. Phys. J. C **80**, 871 (2020).

[36] H. X. Chen, W. Chen, X. Liu, and S. L. Zhu, Sci. Bull. **65**, 1994 (2020).

[37] M. Mikhasenko, L. An, and R. McNulty, arXiv:2007.05501.

[38] X. Y. Wang, Q. Y. Lin, H. Xu, Y. P. Xie, Y. Huang, and X. Chen, Phys. Rev. D **102**, 116014 (2020).

[39] M. Albaladejo, A. N. Hiller Blin, A. Pilloni, D. Winney, C. Fernández-Ramírez, V. Mathieu, and A. Szczepaniak (Joint Physics Analysis Center), Phys. Rev. D **102**, 114010 (2020).

[40] J. Sonnenschein and D. Weissman, arXiv:2008.01095.

[41] R. M. Albuquerque, S. Narison, A. Rabemananjara, D. Rabetiarivony, and G. Randriamanatrika, Phys. Rev. D **102**, 094001 (2020).

[42] J. F. Giron and R. F. Lebed, Phys. Rev. D **102**, 074003 (2020).

[43] L. Maiani, arXiv:2008.01637.

[44] J. M. Richard, arXiv:2008.01962.

[45] J. Z. Wang, D. Y. Chen, X. Liu, and T. Matsuki, arXiv: 2008.07430.

[46] K. T. Chao and S. L. Zhu, Sci. Bull. **65**, 1952 (2020).

[47] G. Yang, J. Ping, and J. Segovia, Symmetry **12**, 1869 (2020).

[48] R. Maciuła, W. Schäfer, and A. Szczurek, Phys. Lett. B **812**, 136010 (2021).

[49] M. Karliner and J. L. Rosner, Phys. Rev. D **102**, 114039 (2020).

[50] Z. G. Wang, arXiv:2009.05371.

[51] X. K. Dong, V. Baru, F. K. Guo, C. Hanhart, and A. Nefediev, arXiv:2009.07795.

[52] Y. Q. Ma and H. F. Zhang, arXiv:2009.08376.

[53] F. Feng, Y. Huang, Y. Jia, W. L. Sang, X. Xiong, and J. Y. Zhang, arXiv:2009.08450.

[54] J. Zhao, S. Shi, and P. Zhuang, Phys. Rev. D **102**, 114001 (2020).

[55] M. C. Gordillo, F. De Soto, and J. Segovia, Phys. Rev. D **102**, 114007 (2020).

[56] R. N. Faustov, V. O. Galkin, and E. M. Savchenko, Phys. Rev. D **102**, 114030 (2020).

[57] X. Z. Weng, X. L. Chen, W. Z. Deng, and S. L. Zhu, arXiv: 2010.05163.

[58] M. A. Shifman, A. I. Vainshtein, and V. I. Zakharov, Nucl. Phys. **B147**, 385 (1979); **B147**, 448 (1979); V. A. Novikov, M. A. Shifman, A. I. Vainshtein, and V. I. Zakharov, Fortschr. Phys. **32**, 585 (1984).

[59] B. L. Ioffe, in *The Spin Structure of the Nucleon*, edited by B. Frois and V. W. Hughes, and N. de Groot (World Scientific, Singapore, 1997).

[60] S. Narison, Cambridge Monogr. Part. Phys., Nucl. Phys., Cosmol. **17**, 1 (2002), arXiv:hep-ph/0205006.

[61] P. Colangelo and A. Khodjamirian, in *At the Frontier of Particle Physics: Handbook of QCD*, edited by M. Shifman, Boris Ioffe Festschrift (World Scientific, Singapore, 2001), Vol. 3, pp. 1495–1576.

[62] M. Nielsen, F. S. Navarra, and S. H. Lee, Phys. Rep. **497**, 41 (2010).

[63] H. Kim and Y. Oh, Phys. Rev. D **72**, 074012 (2005); M. E. Bracco, A. Lozea, R. D. Matheus, F. S. Navarra, and M. Nielsen, Phys. Lett. B **624**, 217 (2005); R. D. Matheus, S. Narison, M. Nielsen, and J. M. Richard, Phys. Rev. D **75**, 014005 (2007).

[64] F. S. Navarra, M. Nielsen, and S. H. Lee, Phys. Lett. B **649**, 166 (2007); S. H. Lee, A. Mihara, F. S. Navarra, and M. Nielsen, Phys. Lett. B **661**, 28 (2008).

[65] J. R. Zhang and M. Q. Huang, J. High Energy Phys. 11 (2010) 057; Phys. Rev. D **83**, 036005 (2011); J. R. Zhang, J. L. Zou, and J. Y. Wu, Chin. Phys. C **42**, 043101 (2018); J. R. Zhang, Phys. Lett. B **789**, 432 (2019); Phys. Rev. D **102**, 054006 (2020); **102**, 074013 (2020).

[66] A. Martínez Torres, K. P. Khemchandani, M. Nielsen, F. S. Navarra, and E. Oset, Phys. Rev. D **88**, 074033 (2013).

[67] K. P. Khemchandani, A. Martínez Torres, M. Nielsen, and F. S. Navarra, Phys. Rev. D **89**, 014029 (2014).

[68] L. J. Reinders, H. R. Rubinstein, and S. Yazaki, Phys. Rep. **127**, 1 (1985).

[69] M. Tanabashi *et al.* (Particle Data Group), Phys. Rev. D **98**, 030001 (2018), and 2019 update.

[70] S. Narison, Phys. Rep. **84**, 263 (1982); G. Launer, S. Narison, and R. Tarrach, Z. Phys. C **26**, 433 (1984); S. Narison, Phys. Lett. B **673**, 30 (2009).